J. Astron. Space Sci. 17(1), 11–18 (2000)

DUST SHELL MODELS FOR THE YOUNG STELLAR OBJECTS IN GIANT MOLECULAR CLOUDS

In-Ok Song and Kyung-Won Suh
Department of Astronomy and Space Science, Chungbuk National University
Cheongju, 361-763, Korea
email: songio@ast.chungbuk.ac.kr, kwsuh@ast.chungbuk.ac.kr

(Received March 30, 2000; Accepted May 2, 2000)

ABSTRACT

We have modeled the observed spectral energy distributions (SEDs) of young stellar objects (YSOs) in giant molecular clouds (GMCs). We propose the theoretical models for the dust envelopes around YSOs. The YSOs in a GMC may share the same initial chemical composition. In this paper, we compare the model SEDs with the observations of the YSOs. Dust shells of the YSOs are composed of a mixture of astronomical silicate and graphite grains. We propose the models for the evolution of the GMCs comparing the shape of the SEDs on the IRAS 2-color diagram with the age.

1. INTRODUCTION

In our Galaxy, stars form in GMCs and large number of YSOs are located in a GMC. It would be useful to make a comparative study of SEDs for YSOs in an individual GMC. The YSOs have thick dust envelopes around them. To model the dust shells around YSOs, we need observed SEDs at infrared range (0.7$\sim$1000μm). The YSOs in a GMC may share the same chemical composition.

We propose the theoretical models of the circumstellar dust envelope that fit the the infrared observations for the YSOs in 2 GMCs; Taurus-Auriga and ρ Ophiuchi. The model results are compared with observed infrared SEDs in individual GMCs. Depending on the dust envelope and central star parameters, the results are very different. We use the IRAS 2-color diagram to discuss the evolution and character of the YSOs in the GMCs compared with the age of GMCs.

2. MODEL CALCULATIONS

For this paper, we have used a numerical code developed by Ivezić & Elitzur (1997) that solves the radiative transfer spherical problem taking full advantage of scaling. We have performed the model calculations in the wavelength range 0.01 to 36000 μm. For dust opacity, we use the opacity for silicate from Ossenkopf et al. (1992), graphite from Draine & Lee (1984), amorphous carbon from Hanner (1988), and SiC from Pégourié (1988). The used initial names are listed in Table 1. The dust size distribution is the one proposed by Mathis et al. (1977) in which grain radii obey $a \geq a_- = 0.005\mu m$ and $a \leq a_+ = 0.25\mu m$. We have assumed a spherical dust shell with the

Table 1. Dust grain opacity functions used for this paper.

Dust	Abbreviation	Reference
warm Silicate	Sil-Ow	Ossenkopf et al. (1992)
graphite	grf-DL	Drain & Lee (1984)
amorphous carbon	amC-Hn	Hanner (1988)
SiC	SiC-Pg	Pègouriè (1988)

density law $\rho(r) \sim r^{-p}$ extending to 10000 times its inner radius (r_c). For simplicity, we assume the temperature at r_c (T_{sub}) is 1500K for all the models. We choose $10\mu m$ as the fiducial wavelength that sets the scale of the optical depth ($\tau_{10\mu m}$). For the central star, a stellar black body temperature (T_c) of 5000K $\sim$ 10000K is used.

3. SED COMPARISONS IN THE INDIVIDUAL GMC

We compare the observed SEDs of 8 YSOs in 2 GMCs with the model results. The data for these stars are taken from the Fourth Catalog of Infrared Observations (Gezari et al. 1998) and the references therein.

From the catalog of Kenyon et al. (1990) and Beichman et al. (1992), we have identified 4 YSOs in Taurus-Auriga with good spectral coverage from near-IR wavelength to far-IR one, including IRAS data. We have selected the four stars that have more detailed observed SEDs for model comparison. Fig. 1 shows the results of the model calculation (line) superimposed on observational data (symbol) for 04112+2803, 04187+1927, 04296+2546, and 04303+2240 in Taurus-Auriga molecular cloud. The SEDs of the YSOs in Taurus-Auriga show that the chemical composition is a mixture of astronomical silicate and graphite grains.

From the catalog of Wilking et al. (1989), we have identified 4 YSOs in ρ Oph with good spectral coverage. Fig. 2 shows the results of the model calculation (line) superimposed on observational data (symbol) for 16372-2347, ρ Oph/IRS14, ρ Oph/IRS23, and 16239-2438. IRS23 seems to be younger than others because the optical depth is thick ($\tau_{10\mu m} = 7.21$) and the absorption feature of silicate is strong.

4. INFRARED 2-COLOR DIAGRAMS

Figure 3 plots 255 YSOs in the IRAS 2-color diagram using [60]-[25] versus [25]-[12]. For Taurus-Auriga (72 objects), the data are from Kenyon et al. (1990). For ρ Ophiuchi (20 objects), the

Table 2. The age and the gradient of IRAS 2-color diagram for the YSOs in 6 GMCs.

GMC	Gradient	Error*	Ref. for the age	Age(yrs)
Taurus-Auriga (116)	0.68	0.32	Kenyon et al. (1990)	$1 \sim 2 \times 10^5$
ρ Ophiuchi (64)	-0.53	0.16	Wilking et al. (1989)	$3.9 \pm 1.2 \times 10^5$
Chamaeleon I (47)	0.02	0.24	Prusti et al. (1992a)	5×10^5
Chamaeleon II (41)	0.36	0.21	Lawson et al. (1996)	$10^5 \sim 10^7$
Monoceros OB1 (28)	0.26	0.18	Hughes & Hartigan (1992)	9×10^5
Lynds 1641 (123)	0.86	0.19	Strom et al. (1989)	6×10^6

* Error of the gradient by standard deviation.

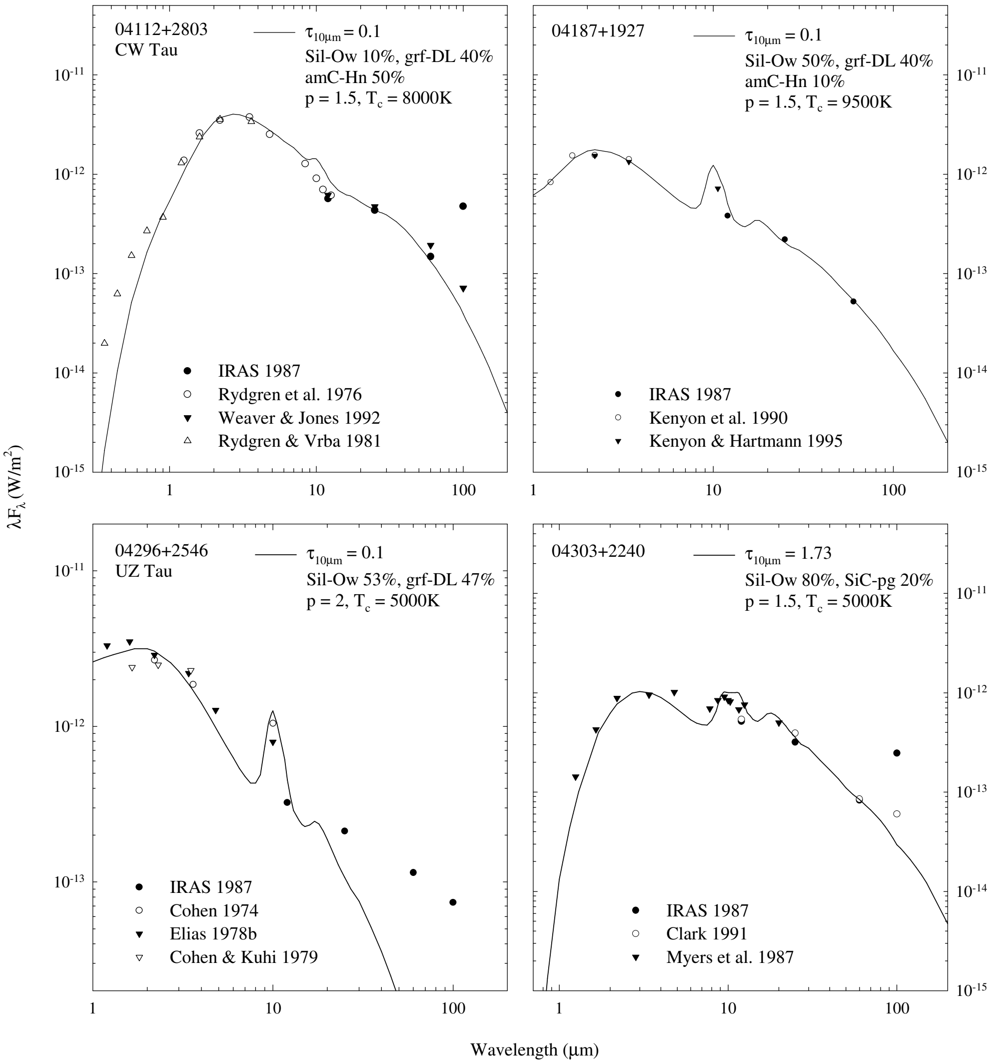

Figure 1. SED Comparisons for the YSOs in Taurus-Auriga molecular cloud.

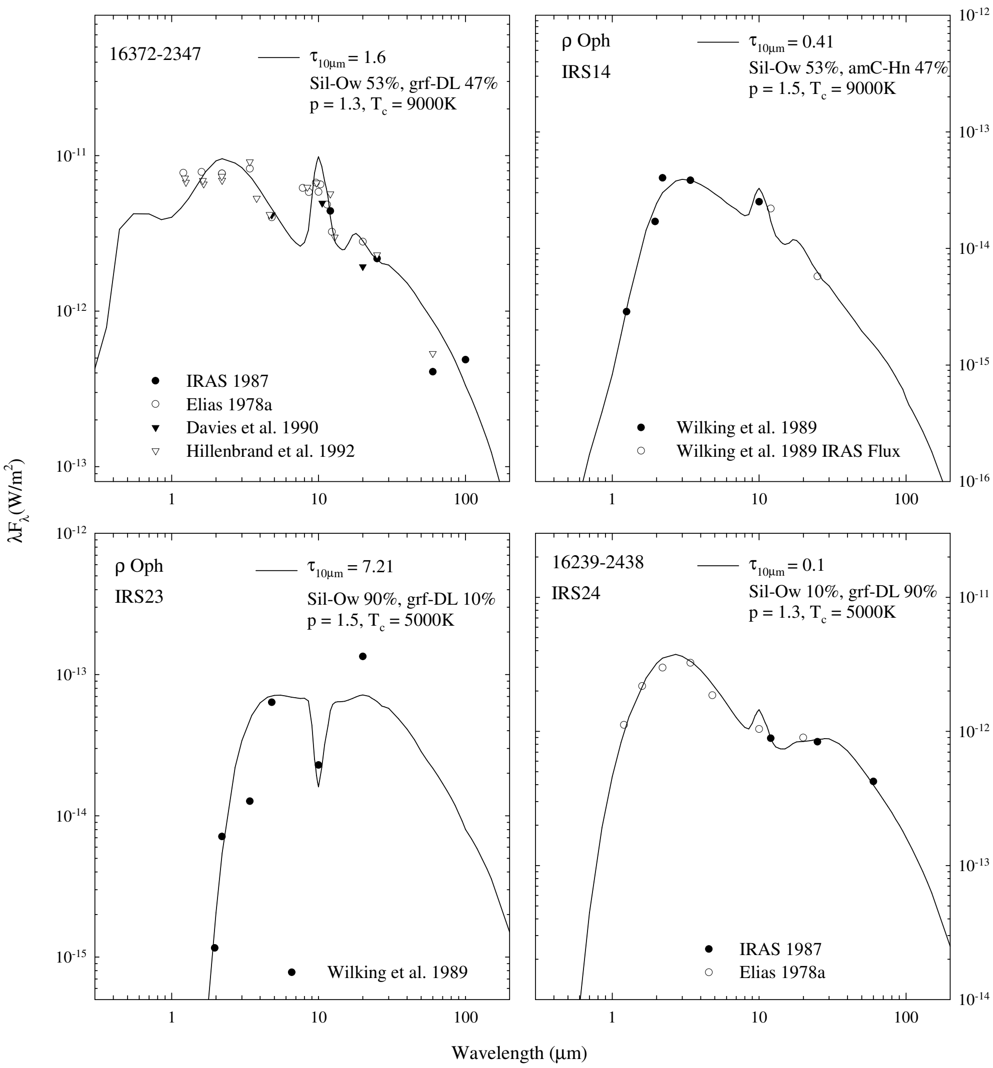

Figure 2. SED Comparisons for the YSOs in ρ Ophiuchi molecular cloud.

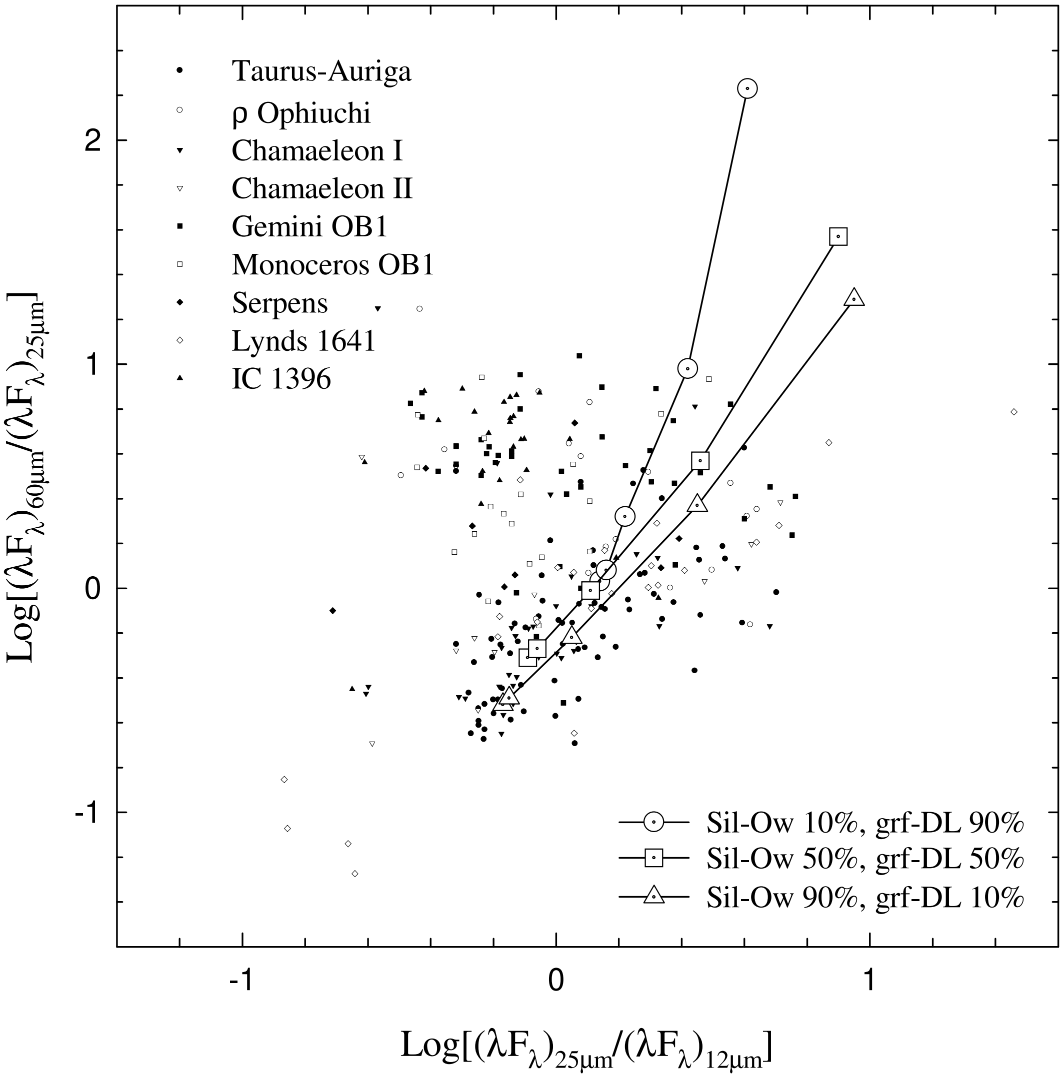

Figure 3. The IRAS 2-color diagram for YSOs.

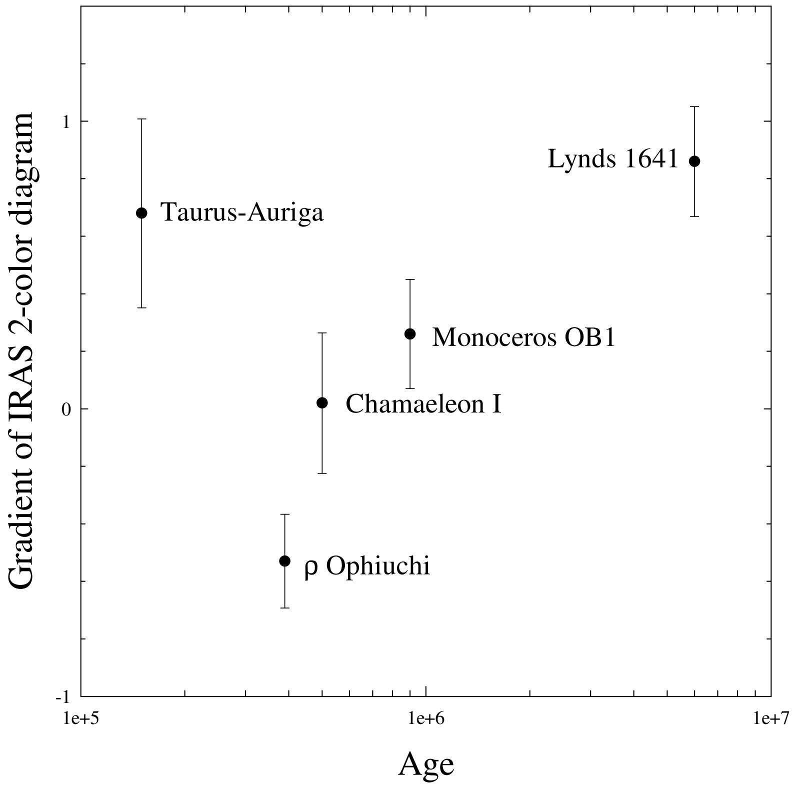

Figure 4. Evolution of the GMCs.

data are from Wilking et al. (1989). For Chamaeleon I (33 objects), the data are from in Prusti et al. (1992a). For Chamaeleon II (10 objects), the data are from in Prusti et al. (1992b). For Gemini OB1 (41 objects), the data are from in Carpenter et al. (1995). For Monoceros OB1 (51 objects), the data are from in Margulis et al. (1989). For Serpense (8 objects), the data are from in Zhang et al. (1988). For Lynds 1641 (26 objects), the data are from in Strom et al. (1989). For IC 1396 (24 objects), the data are from in Schwartz et al. (1991). Stars with only upper limits at any wavelength are not used. In Figure 3, the small symbols are the observational data and the lines with large symbols are the model calculations for a range in the dust shell optical depth ($\tau_{10\mu m}$ = 0.1, 0.41, 1.73, 7.21, and 30). All models assume the same central black body temperature (5000K) and the dust density distribution of $r^{-1.5}$. The more silicate grains correlatively in which they composed of dust envelope with graphite grains, the more gentle gradient of position of YSO in this diagram.

We are concerned about the relation between the gradient of the GMC in the IRAS 2-color diagram and the age as well as the feature of dust grains. From Figure 3, we find the first square fitting gradient for individual objects in each GMC. Table 2 lists the gradient in the IRAS 2-color diagram and the age estimated by other authors. Figure 4 shows their relations. From Figure 4, we roughly find the general tendency that the GMC showing the steeper gradient is older than others.

5. SUMMARY

We have made the radiative transfer models for the dust envelops around YSOs. Depending on the parameters of the dust envelope and the central star, the results are very different. We have compared the observed SEDs of the YSOs in 2 GMCs – Taurus-Auriga and ρ Ophiuchi – with the model results. Dust shells of the YSOs in both of the GMCs are composed of a mixture of astronomical silicate and graphite grains. We recognized the different shapes in the IRAS 2-color diagram of the YSOs for each GMC. As a difference of the first square fitting gradient for each GMC, we roughly find the general tendency that the GMCs showing steeper gradient are older than others.

ACKNOWLEDGEMENTS: This research was supported by the Chungbuk National University Basic Science Research Fund (BSRI-00-S11).

REFERENCES

Beichman, C. A., Boulanger, F., & Moshir, M. 1992, ApJ, 386, 248
Carpenter, J. M., Snell, R. L., & Schloerb, F. P. 1995, ApJ, 450, 201
Clark, F. O. 1991, ApJS, 75, 611
Cohen, M. 1974, MNRAS, 169, 257
Cohen, M., & Kuhi, L. O. 1979, ApJS, 41, 743
Davies, J. K., Evans, A., Bode, M. F., & Whittet, D. C. B. 1990, MNRAS, 247, 517
Draine, B. T., & Lee, H. M. 1984, ApJ, 285, 89
Elias, J. H. 1978a, ApJ, 224, 453
Elias, J. H. 1978b, ApJ, 224, 857
Gezari, D. Y., Schmitz, M., Pitts, P. S., & Mead, J. M. 1998, Catalog of Infrared Observation, Fourth Edition, NASA Reference Publication 1294
Hanner, M. S. 1988, NASA Conf. Pub., 3004, 22
Hillenbrand, L. A., Strom, S. E., Vrba, F. J., & Keene, J. 1992, ApJ, 397, 613
Hughes, J., & Hartigan, P. 1992, AJ, 104, 680
Infrared Astronomical Satellite (IRAS) Catalogs and Atlases: Explanatory Supplement 1987, ed. L. Brotzman (Astronomical Data Center)
Ivezić, A., & Elitzur, M. 1997, MNRAS, 287, 799
Kenyon, S. J., & Hartmann, L. 1995, ApJS, 101, 117
Kenyon, S. J., Hartmann, L. W., Strom, K. M., & Strom, S. E. 1990, AJ, 99, 869
Lawson, W. A., Feigelson, E. D., & Huenemoerder, D. P. 1996, MNRAS, 280, 107
Margulis, M., Lada, C. J., & Young, E. T. 1989, ApJ, 345, 906
Mathis, J. S., Rumpl, W., & Nordsieck, K. H. 1977, ApJ, 217, 425
Myers, P. C., Fuller, G. A., Mathieu, R. D., Beichman, C. A., Benson, P. J., Schild, R. E., & Emerson, J. P. 1987, ApJ, 319, 340
Ossenkopf, V., Henning, Th., & Mathis, J. S. 1992, A&A, 261, 567
Pégourié, B. 1988, A&A, 194, 335
Prusti, T., Whittet, D. C. B., & Wesselius, P. R. 1992a, MNRAS, 254, 361
Prusti, T., Whittet, D. C. B., Assendorp, R., & Wesselius, P. R. 1992b, A&A, 260, 151
Rydgren, A. E., Strom, S. E., & Strom, K. M. 1976, ApJS, 30, 307
Rydgren, A. E., & Vrba, F. J. 1981, AJ, 86, 1069
Schwartz, R. D., Gyulbudaghian, A. L., & Wilking, B. A. 1991, ApJ, 370, 263

Strom, K. M., Newton, G., Strom, S. E., Seaman, R. L., Carrasco, L., Cruz-Gonzalez, I., Serrano, A., & Grasdalen, G. L. 1989, ApJS, 71, 183
Weaver, W. B., & Jones, G. 1992, ApJS, 78, 239
Wilking, B. A., Lada, C. J., & Young, E. T. 1989, ApJ, 340, 823
Zhang, C. Y., Lqureijs, R. J., Colark, F. O., & Wesselius, P. R. 1988, A&A, 199, 170